Energy Conversion and Management 121 (2016) 402–408

Contents lists available at ScienceDirect

Energy Conversion and Management

journal homepage: www.elsevier.com/locate/enconman

Ash behavior during hydrothermal treatment for solid fuel applications. Part 1: Overview of different feedstock

Mikko Mäkelä [a,b,*], Andrés Fullana [c], Kunio Yoshikawa [a]

[a] Tokyo Institute of Technology, Department of Environmental Science and Technology, G5-8, 4259 Nagatsuta-cho, Midori-ku, Yokohama 226-8502, Japan
[b] Swedish University of Agricultural Sciences, Department of Forest Biomaterials and Technology, Skogsmarksgränd, 90183 Umeå, Sweden
[c] University of Alicante, Department of Chemical Engineering, PO Box 99, 03080 Alicante, Spain

ARTICLE INFO

Article history:
Received 22 March 2016
Received in revised form 5 May 2016
Accepted 5 May 2016
Available online 13 May 2016

Keywords:
Biomass
Char
Hydrothermal carbonization
Principal component analysis
Waste
Wet torrefaction

ABSTRACT

Differences in ash behavior during hydrothermal treatment were identified based on multivariate data analysis of literature information on 29 different feedstock. In addition, the solubility of individual elements was evaluated based on a smaller data set. As a result two different groups were distinguished based on char ash content and ash yield. Virgin terrestrial and aquatic biomass, such as different types of wood and algae, in addition to herbaceous and agricultural biomass, bark, brewer's spent grain, compost and faecal waste showed lower char ash content than municipal solid wastes, anaerobic digestion residues and municipal and industrial sludge. Lower char ash content also correlated with lower ash yield indicating differences in chemical composition and ash solubility. Further evaluation of available data showed that ash in industrial sludge mainly contained anthropogenic Al, Fe and P or Ca and Si with low solubility during hydrothermal treatment. Char from corn stover, miscanthus, switch grass, rice hulls, olive, artichoke and orange wastes and empty fruit bunch had generally higher contents of K, Mg, S and Si than industrial sludge although differences existed within the group. In the future information on ash behavior should be used for enhancing the fuel properties of char based on feedstock type and hydrothermal treatment conditions.

1. Introduction

Hydrothermal treatment can be used for upgrading a wide variety of biomass and waste feedstock for solid fuel applications. Thermochemical conversion in hot compressed water under relatively low temperature and self-generated pressure can offer several advantages over other processing routes. Hydrothermal treatment enables robust operation, high energy efficiency, relatively high yields and the production of direct replacements for existing solid fuels [1,2]. In addition, no prior drying of a feedstock is required making hydrothermal processes ideal for wet materials such as agricultural and forest residues or municipal and industrial waste biomass [3,4]. Material handling and drying properties are simultaneously enhanced [5,6] generating significant cost savings during handling, storage and transport of attained hydrochar.

Although hydrothermal treatment has been reported already in the early 20th century as a method for simulating natural coalification [7], the wealth of published information has increased considerably during the last 5 years [8]. It is currently considered well known that reaction temperature governs char properties mainly through hydrolysis, dehydration, decarboxylation and aromatization of organic components [9–11]. The characteristics of subcritical water resemble those of organic solvents at room temperature and favor reactions normally catalyzed by acids and bases [1,12]. Oxygen and volatile contents of the solid are decreased followed by an increase in energy densification and hydrophobicity [2,9]. Depending on the feedstock and prevailing process conditions, hydrothermal treatment can be used for producing solid fuels that approach the characteristics of low rank natural coals.

Hydrothermal treatment leads to partial dissolution of inorganic components and has been reported to enable nitrogen and chlorine removal from municipal solid waste (MSW) [4]. Properties of subcritical water and production of organic acids during hydrothermal treatment increase the solubility of alkali and alkaline earth metals [13,14]. Manipulation of ash content and composition of a solid is a major benefit for fuel production as it can increase energy densification, improve slagging and fouling

* Corresponding author at: Tokyo Institute of Technology, Department of Environmental Science and Technology, G5-8, 4259 Nagatsuta-cho, Midori-ku, Yokohama 226-8502, Japan.
E-mail addresses: makela.m.aa@m.titech.ac.jp, mikko.makela@slu.se (M. Mäkelä).

http://dx.doi.org/10.1016/j.enconman.2016.05.016
0196-8904/

behavior during combustion, and decrease corrosion of process equipment [15,16]. Previously, equal or improved slagging, fouling or alkali indices have been reported for hydrothermally treated energy crops and agricultural residues [17,18]. In addition, removal of alkali metals was recently reported to improve combustion properties of a variety of treated biomass and waste feedstock [19].

Behavior of ash components varies based on feedstock and hydrothermal treatment conditions. Even though the number of published information in the field has been expanding, no comprehensive reports exist on ash behavior from different biomass and waste feedstock under a wide range of treatment conditions. This work was divided into two separate parts. The objective of this first part was to identify differences in ash behavior based on feedstock type. Literature data on individual experiments on various feed materials were compiled, reviewed and interpreted using multivariate data analysis. In addition, the solubility of individual elements was evaluated based on a smaller data set. The second part of this work focuses on determining the effect of treatment conditions on ash properties of industrial waste biomass using univariate regression techniques. Overall the attained results will help in understanding ash behavior during hydrothermal treatment of different biomass and waste feedstock for solid fuel applications.

2. Materials and methods

2.1. Data compilation and review

Experimental data on the effects of hydrothermal treatment temperature, retention time and reactor solid load on char ash content, mass yield, energy densification and energy yield were compiled from relevant literature reports. Papers that did not report the ash contents of the feed and attained char samples were excluded. Papers that failed to include mass yield, energy densification or energy yield, but allowed respective estimation based on given information were however included. In addition, previously unpublished data on char ash from ref. [10] was taken into account. The final data set included 206 individual experiments on 29 different feedstock (Table 1). The data set was not exhaustive, but provided an overview of different feedstock used in the hydrothermal treatment field.

Compiled data were revised to enable comparison between different experiments. Retention time was expressed in hours (h) and was log10 transformed. Reactor solid load was expressed as a weight percentage (%) of the combined mass of added liquid and the feed on a dry basis (db). If no liquid was added solid load was taken as the dry solids content (%) of the feed. Ash yield was calculated as:

$$\text{Ash yield}\ (\%, \text{db}) = \left(\frac{ac_{hc}}{ac_f} \cdot \text{MY}\right) \cdot 100\% \quad (1)$$

where ac_{hc} and ac_f denoted the ash contents (db) of char and the feed, respectively, and MY char mass yield (db). To separate between the dissolution of organic and ash components, final mass yield was expressed on a dry, ash-free (daf) basis:

$$\text{Mass yield}\ (\%, \text{daf}) = \left(\text{MY} \cdot \frac{1 - ac_f}{1 - ac_{hc}}\right) \cdot 100\% \quad (2)$$

Table 1
Information on different feedstock and treatment conditions included in the overview.

Index	Feedstock	Refs.	Treatment temperature (°C)	Retention time (h)	Solid load (%)[a]	Additive	Reactor size (L)	No. of compiled data points
1	Oak wood	[19]	200–250	1.0	10		0.6	2
2	Loblolly pine	[20–22]	200–280	0.1–0.5	9.1–17		0.1	14
3	Coniferous wood	[23]	180–250	3.0–6.0	11–14		1.0	15
4	Eucalyptus bark	[24]	220–300	2.0–10	9.1		0.1	8
5	Willow	[19]	200–250	1.0	10		0.6	2
6	Miscanthus	[17,19,25]	190–260	0.1–1.0	10–17		0.1–0.6	8
7	Switch grass	[17]	200–260	0.1	17		0.1	3
8	Corn stover	[17]	200–260	0.1	17		0.1	3
9	Rice hulls	[17]	200–260	0.1	17		0.1	3
10	Maize silage	[26]	200–260	0.3–10	6.7		1.0	9
11	Wheat straw	[27]	200–260	6.0	4.8	Acetic acid and potassium hydroxide	1.0	22
12	Macroalgae	[19,28]	180–250	1.0–16	4.8–17	Citric acid [28]	0.1–0.6	18
13	Microalgae	[19]	200–250	1.0	10		0.6	2
14	Olive waste	[18]	200–250	2.0–24	29		1.0	6
15	Artichoke waste	[18]	200–250	2.0	14		1.0	3
16	Orange waste	[18]	200–250	2.0	21		1.0	3
17	Empty fruit bunch	[29]	100–260	0.5	9.1		0.5	4
18	Brewer's spent grain	[30]	200–240	14	12	Citric acid	0.2	2
19	Greenhouse waste	[19]	200–250	1.0	10		0.6	2
20	Food waste	[19,31]	200–250	1–16	10–20		0.2–0.6	3
21	Paper	[31]	250	16	20		0.2	1
22	MSW fiber	[19]	200–250	1.0	10		0.6	2
23	MSW	[31,32]	225–250	1.5–16	20–67		0.2 and 3.0 m^3	2
24	Compost	[33]	180–250	1.0–8.0	7.0		0.1	9
25	Faecal waste	[34]	180–200	0.5–2.0	4.5		N/A	6
26	Sewage sludge	[19,34,35]	160–200	0.5–1.0	3.4		N/A	21
27	Anaerobic digestion residue	[19,31]	200–250	1.0–16	10–20		0.2–0.6	3
28	Mixed sludge[b]	[36]	180–260	0.5–5	21	Hydrogen chloride and sodium hydroxide	1.0	15
29	Paper sludge[b]	[10]	180–260	1.0–6.3	13–20		1.0	15

N/A = not available.
[a] Weight percentage of the combined mass of liquid and the feed on a dry basis.
[b] From pulp and paper mills.

In a comparable way energy densification was expressed as:

$$\text{Energy densification (daf)} = \frac{HV_{hc}}{HV_f} \quad (3)$$

where HV_{hc} and HV_f described the heating values (MJ kg^{-1}, daf) of char and the feed, respectively. If needed the HVs were revised to daf basis by correcting for respective ash contents. Char energy yield was then calculated as:

$$\text{Energy yield (\%)} = (MY \cdot ED) \cdot 100\% \quad (4)$$

where MY and ED respectively denoted char mass yield and energy densification and were both given dimensionless on a daf basis. The 206×8 data set, containing individual experiments as row objects and reaction temperature, retention time, solid load, ash content, ash yield, mass yield, energy densification and energy yield as the corresponding columns, is given in Table A.1 (Supplementary information).

A second smaller data set on feedstock type and ash composition was also compiled based on unpublished data from [10,36] and refs. [17,18,29]. The data included 44 experiments on corn stover, miscanthus, switch grass, rice hulls, olive waste, artichoke waste, orange waste, empty fruit bunch, mixed sludge and paper sludge. Char ash content, ash yield and elemental composition were included as variables. In addition, 10 observations describing the untreated feedstock were considered. The compositional data from [10,18,29,36] were revised to elemental basis and assumed to constitute 100% of sample ash. The second 54×13 data set is provided in Table A.2.

2.2. Data interpretation

The compiled multivariate data were interpreted through principal component analysis. The data sets were decomposed according to a general principal component model:

$$\mathbf{X} = \sum_{i=1}^{n} \mathbf{t_i} \mathbf{p_i^T} + \mathbf{E_n} \quad (5)$$

where $\mathbf{X}$ denoted a preprocessed data matrix containing individual experiments as row objects and measured or calculated variables as the corresponding columns. The vectors $\mathbf{t_i}$ and $\mathbf{p_i}$ described the respective principal component scores and orthonormal variable loadings and $\mathbf{E_n}$ the residual matrix after n components. Both data sets were preprocessed by subtracting the mean and dividing by the standard deviation of each column to enable comparison between variables given in different units. Data rank and the number of principal components included in the models were determined based on the minima of root mean squared errors (RMSE) of cross validation:

$$\text{RMSE} = \sqrt{\frac{\sum_{i=1}^{m} (y_i - \hat{y}_i)^2}{m}} \quad (6)$$

where y_i and $\hat{y}_i$ denote the observed and predicted values, respectively, and m the number of cross validation objects. The cross validation sets were constructed by splitting the data into 10 consecutive subgroups of one object. Each subgroup was then tested with a prediction model based on the remaining objects until all objects had been tested once. Hotelling T^2, residual sum of squares Q and statistical significance limits of grouped data were used to evaluate model performance and differences between groups. A detailed description of the calculation of these parameters can be found from Jackson [37]. Calculations and data plotting were performed with the Matlab® (The MathWorks, Inc.) and OriginLab® (OriginLab Corp.) software packages.

3. Results

According to the first data set a majority of hydrothermal experiments were performed within a temperature range 180–260 °C with an isothermal retention time equal or less than 14 h. Most experimenters also used low reactor solid loads as 90% of the observations were within 4.3–21%. Ash contents of attained char ranged from 0.2% to 82% due to the wide variety of different feedstock types. With 18 individual observations on loblolly pine, rice hulls, eucalyptus bark, MSW fiber, MSW, sewage sludge or paper sludge calculated char ash yields exceeded 100% likely due to uncertainties in char sampling. A majority of char mass yields (daf) ranged from 30% to 86% with a mean of 54%. Char energy densification (daf) was in the range 0.7–2.0 as 90% of the observations were within 1.0–1.7. The majority of reported or calculated energy yields ranged from 43% to 95% as only two observations exceeded 100% (Table 2). Individual experiments with deviating ash yield, energy densification or energy yield values were not excluded as the presence of outliers was further evaluated based on determined principal components.

Three principal components, which explained a total of 73% of variation in the data, were chosen for the first data set. As could be expected the data seemed slightly noisy. Two observations were identified as outliers and were excluded from the data. The outliers reported hydrothermal treatment of sewage sludge and a pilot-scale investigation on treatment of MSW. No meaningful structure was found from the remaining model residuals. Variable loadings and scores based on the first three principal components are presented in Fig. 1. Hotelling T^2, residual sum of squares Q and a scree plot after the removal of outliers are given in Figs. A.1 and A.2 (Supplementary information).

4. Discussion

4.1. Ash content and yield

Larger data sets often require more advanced data analysis than just means, standard deviations and correlations. Principal compo-

Table 2
Overview of the first data set.

Property	Temp. (°C)	Time (h)[a]	Load (%)	Ash (%, db)	Ash yield (%, db)	Mass yield (%, daf)	Energy densification (daf)	Energy yield (%)
Range	100–300	0.08–24.0	3.41–66.8	0.22–81.5	4.30–121	17.3–94.6	0.69–2.01	25.7–107
Mean	217	3.42	11.9	17.8	59.2	53.9	1.28	66.8
Std	32.0	3.94	7.35	19.6	30.4	16.8	0.22	16.0
5th–95th percentile range	180–260	0.08–14	4.30–20.5	0.50–55.8	11.9–107	30.2–86.2	1.02–1.67	43.0–94.6

db = dry basis.
daf = dry, ash-free.
std = standard deviation.
[a] Retention time was log10 transformed for the final data matrix.

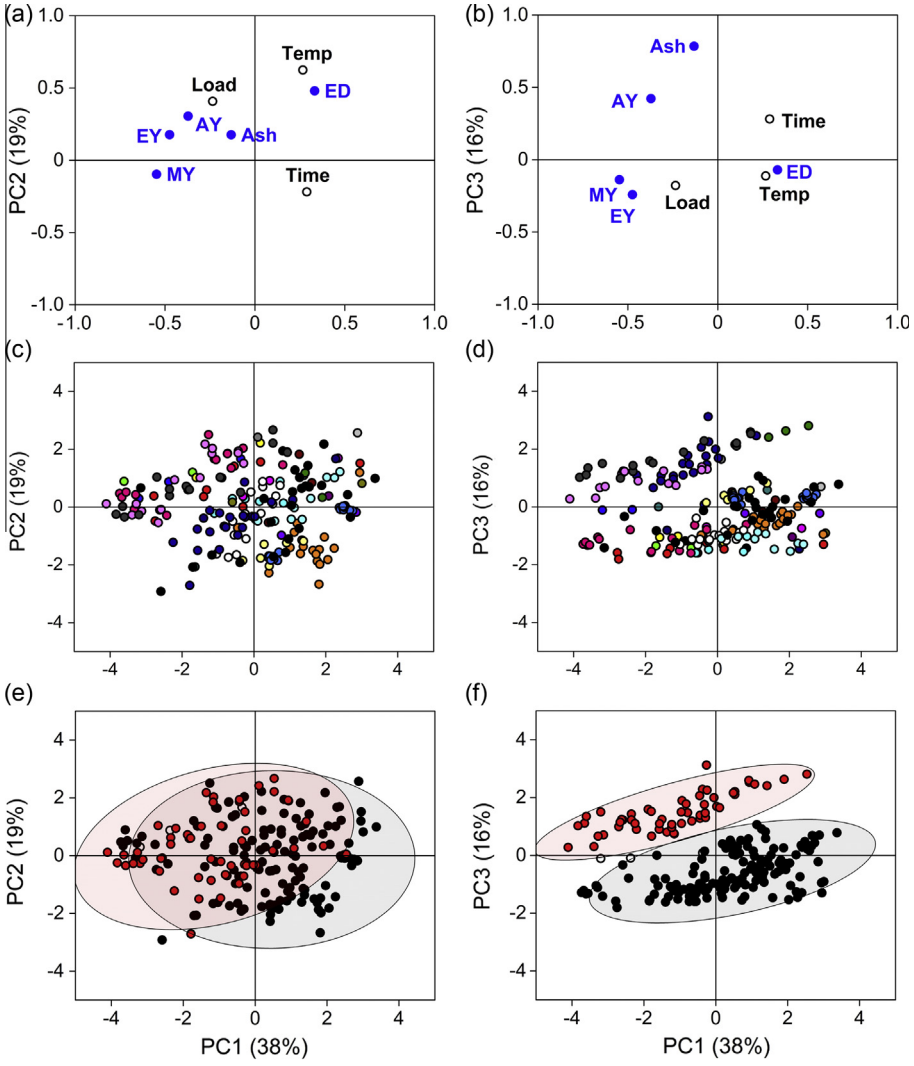

Fig. 1. Variable loadings (a and b) and object scores (c and d) based on the first three principal components. In (c and d) scores were colored based on feedstock type and in (e and f) the objects were classified to two groups with ellipses denoting 95% probability. Three unfilled symbols were left unclassified. Temp: treatment temperature (°C), Time: retention time (log10 h), Load: reactor solid load (%), Ash: char ash content (%, db), AY: ash yield (%, db), MY: mass yield (%, daf), ED: energy densification (daf) and EY: energy yield (%). (For interpretation of the references to color in this figure legend, the reader is referred to the web version of this article.)

nents are very useful in describing correlations and groupings in multivariate data and in decreasing data dimensions to simplify interpretation [38,39]. In addition, principal components can decrease data uncertainty from experimental errors by including only components that facilitate interpretation of systematic variation. As illustrated in Fig. 1a, the first principal component explained 38% of variation in the data and included mainly the effects of treatment temperature and retention time on char ash, mass and energy yield and energy densification. Increased temperature and retention time correlated with decreased yields and increased energy densification. Several correlations describing the effects of treatment temperature and retention time on dissolution of organic components have previously been proposed [9,40]. In addition, the effects and statistical significance of temperature and time on the properties of char from sewage and paper sludge have recently been determined based on univariate regression models [10,35]. Bach et al. [41] described these effects through the Arrhenius' equation, where reaction rate is exponentially dependent on treatment temperature but directly dependent on retention time.

The second principal component explained mainly the contrasting effects of treatment temperature and reactor solid load and covered 19% of variation in the data (Fig. 1a). Based on the results, reactor solid load had a positive effect on char energy yield. Thus far most laboratory studies have reported low reactor solid loads likely as an attempt to explain reaction mechanisms and maximize the carbon content of attained char. A comparison between hydrothermal and vapothermal treatment based on reactor solid load was reported for wheat straw and an anaerobic digestion (AD) residue [42]. The authors concluded that the use of higher solid loads decreased carbon losses to the liquid, but produced a solid with a lower final carbon content. As illustrated in Fig. 1c, no clear groupings in char properties between different feedstock were observed based on the first two principal components.

Differences in char ash content and ash yield were included in the third principal component (Fig. 1b), which explained 16% of data variation. The results showed that char ash contents were different between different feedstock types. In addition, higher ash contents led to higher ash yields, which indicated differences in chemical composition and ash solubility. As shown in Fig. 1d, two separate groups of feedstock could be distinguished. The larger group lower in the vertical axis included char produced from virgin terrestrial and aquatic biomass, such as different types of wood and algae, in addition to herbaceous and agricultural biomass,

bark, brewer's spent grain, compost and faecal waste. The smaller group higher on the vertical axis was composed of char from higher ash feeds, such as MSW, AD residues and sludge produced by municipal and industrial wastewater treatment plants, which also showed higher ash yields than those in the lower group. To verify these differences, scores of the first three principal components were classified in two different groups (Fig. 1e and f). As indicated by Fig. 1f, the groups were statistically different based on char ash content and yield. Only three observations on rice hulls were left unclassified due to uncertainty based on the two groups. It should be noted that initial liquid pH was also included as variable during preliminary calculations, but did not enhance the model or data interpretation and was hence excluded from the final data set. A correlation matrix of the data set and a loadings plot of the first three principal components are given in Table A.3 and Fig. A.3.

4.2. Ash composition

To clarify potential correlation between feedstock type and ash composition a smaller data set on corn stover, miscanthus, switch grass, rice hulls, olive, artichoke and orange wastes, empty fruit bunch, mixed sludge and paper sludge was compiled based on refs. [10,17,18,29,36]. The data included char ash content, ash yield and respective elemental composition. Observations on untreated feedstock and even elements with low concentrations were also included. Based on the reports, ash content and composition were determined through loss on ignition at 550 °C for 8 h followed by with X-ray fluorescence (XRF) spectroscopy, respectively, or at 575 °C for 24 h followed by scanning electron microscopy with an energy dispersive X-ray detector. Only one ref. reported the use of an XRF spectrometer without prior details on determination of ash contents. A principal component model indicated that the first four components explained 82% of total variation. A correlation matrix is given in Table A.4.

A meaningful interpretation was already provided by the first three principal components. As illustrated in Fig. 2, the first principal component included variation in ash content and ash yield and provided a clear separation between feedstock types according to the previously defined two groups. Chars produced from industrial sludge had higher ash content and ash yield. Char from mixed sludge showed higher contents of ash Al, Fe and P, as char from paper sludge showed comparatively higher ash Ca and Si. It should be noted that the Ti contents of all samples were low, generally within 1–2% of sample ash. Within the pulp and paper industry high Al, Fe and P contents in mixed or pure biosludge from wastewater treatment are generally derived from the use of cationic polymers in sludge conditioning or addition of phosphoric acid for supporting bacteria [43]. In addition, high Ca contents in paper sludge likely originate from the use of paper coating agents such as calcium carbonate [44], which has showed low solubility during hydrothermal treatment for solid fuel production [10].

Char from rice hulls that previously remained unclassified had higher ash content and ash yield but similar ash composition as compared to chars produced from corn stover, miscanthus, switch grass, and empty fruit bunch (Fig. 2c and d). These chars and their respective feedstock generally had higher K and Si content than industrial sludge. The second and third principal components mainly separated ash composition within the individual groups. As an example char from olive, artichoke, and orange wastes showed lower Si but higher K, Mg and S than char from corn stover, miscanthus, switch grass, rice hulls or empty fruit bunch. In general Si based minerals are common structural components of plant tissues or can derive from soil and sand particle contamination during harvesting, transportation or handling of biomass and waste feedstock. Based on previous reports Si has also exhibited low solubility during hydrothermal treatment [10,17]. As discussed by Reza et al. [17], a majority of Ca and K in virgin lignocellulosic biomass is associated with hemicellulose or extractives of which especially hemicellulose is readily soluble under hydrothermal conditions. Based on the data olive waste and mixed sludge chars had the highest P contents, which generally increased through hydrothermal treatment. Similar effects were observed by Benavente et al. [18] and have also been reported for several animal manures [45,46] suggesting low solubility of phosphate salts and apatite during hydrothermal treatment. Highest Na and Cl contents were reported for chars produced from artichoke waste and empty fruit bunch.

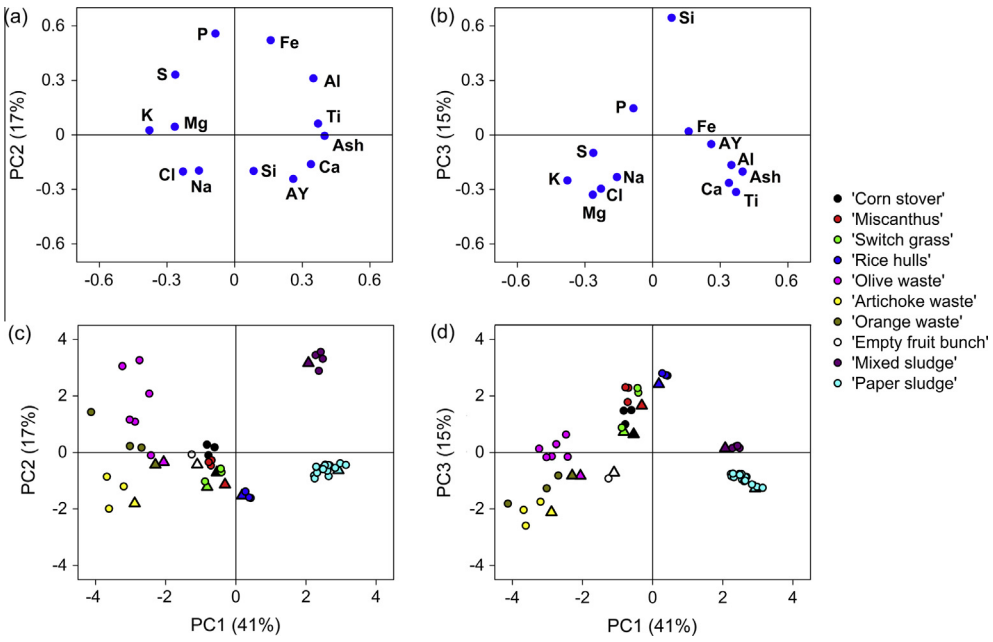

Fig. 2. Variable loadings (a and b) and object scores (c and d) based on the first three principal components of the second data set [10,17,18,29,36]. In (c and d) larger triangular symbols denote untreated feedstock. Ash: char ash content (%, db) and AY: ash yield (%, db).

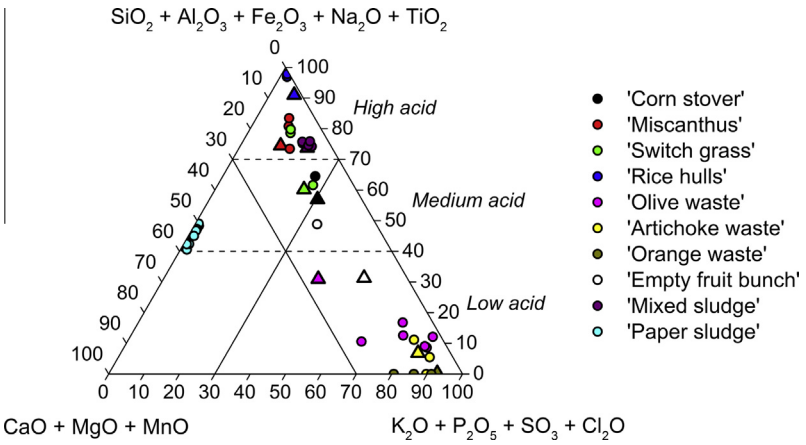

Fig. 3. Ash composition of char samples produced from different feedstock [10,17,18,29,36] based on the classification system of Vassilev et al. [47,48]. Larger triangular symbols denote untreated feedstock.

Differences in ash composition were further evaluated based on potential behavior during char combustion. The compositional data in [17] were corrected to respective oxides. Various parameters based on the ratio of acidic and basic oxides have long been used for estimating potential ash behavior during coal combustion. These parameters have also been implemented for biomass in lack of better alternatives [15,16]. It is currently widely accepted that an increasing share of basic components, such as Ca, Fe, Mg, Na and K bearing minerals, results in lower ash melting temperatures and can cause problems during coal combustion. However, recently Vassilev et al. [47,48] provided an extensive discussion on the properties of biomass ash and found that its fusion behavior was more variable than that of coal. Based on their results, Ca, Al and Ti increased ash deformation temperatures and mainly medium to high contents of K and Si governed the formation of low temperature eutectics. The authors proposed a new classification system to enhance preliminary predictions on ash behavior for solid biomass fuels. Observations included in the second data set were evaluated based on this classification and are illustrated in Fig. 3.

Chars produced from corn stover, miscanthus, switch grass, rice hulls and mixed sludge were located within a group of herbaceous and agricultural biomass with medium to high acid tendencies (Fig. 3). These materials were expected to have low to medium (or in some cases high) ash fusion temperatures [48], which were also generally increased through hydrothermal treatment. Chars from olive, artichoke and orange wastes and empty fruit bunch were analogous to herbaceous and agricultural residues with low to medium acid tendencies and lower ash fusion temperatures [48]. The acid tendency of especially olive wastes was also decreased through hydrothermal treatment as the opposite was observed for empty fruit bunch (Fig. 3). In general, biomass varieties with lower ash fusion temperatures were located to the right in the ternary diagram [48] and would more likely cause problems during combustion. The properties of char from paper sludge were similar to those of herbaceous and agricultural biomass, contaminated biomass and to some extent wood and woody biomass. These biomass types normally showed higher Ca and lower Na and P contents with medium to high ash fusion temperatures [48]. No considerable differences between char samples from industrial sludge were observed due to the low solubility of ash components. Although detailed information on combustion conditions coupled with fuel and ash compositions is required for reliably predicting behavior during combustion [16,47,48], ash classification can provide useful proximate estimations on potential behavior during combustion. In the future such information should be used for enhancing the combustion properties of char based on feedstock type and hydrothermal treatment conditions.

5. Conclusions

Ash behavior during hydrothermal treatment depends on feedstock type and treatment conditions. Two different groups were identified out of 29 different feeds based on char ash content and ash yield. Virgin terrestrial and aquatic biomass, such as different types of wood and algae, in addition to herbaceous and agricultural biomass, bark, brewer's spent grain, compost and faecal waste showed lower char ash content and ash yield compared to MSW, AD residues and municipal and industrial sludge indicating differences in chemical composition and ash solubility. Further evaluation of available data showed that ash in industrial sludge contained mainly anthropogenic Al, Fe and P or Ca and Si, which showed low solubility. Char from corn stover, miscanthus, switch grass, rice hulls and olive, artichoke and orange wastes and empty fruit bunch had generally higher contents of K, Mg, S and Si compared to industrial sludge although differences existed within the group. Differences in ash behavior are relevant as they affect char properties for solid fuel applications. In the future this information should be used for enhancing the combustion properties of char based on feedstock type and hydrothermal treatment conditions. The second part of this work will focus on determining the effect of treatment conditions on ash properties of paper sludge.

Acknowledgements

The contribution of Prof. Paul Geladi from the Swedish University of Agricultural Sciences in proof reading this work is greatly appreciated. The Finnish Foundation for Technology Promotion mainly funded this work as a Postdoctoral Fellowship through the Foundations' Post Doc pool.

Appendix A. Supplementary material

Supplementary data associated with this article can be found, in the online version, at http://dx.doi.org/10.1016/j.enconman.2016.05.016.

References

[1] Peterson AA, Vogel F, Lachance RP, Fröling M, Antal Jr MM, Tester JW. Thermochemical biofuel production in hydrothermal media: a review of sub- and supercritical water technologies. Energy Environ Sci 2008;1:32–65. http://dx.doi.org/10.1039/b810100k.

[2] Libra JA, Ro KS, Kammann C, Funke A, Berge ND, Neubauer Y, et al. Hydrothermal carbonization of biomass residuals: a comparative review of the chemistry, processes and applications of wet and dry pyrolysis. Biofuels 2011;2:71–106. http://dx.doi.org/10.4155/BFS.10.81.

[3] Ho DP, Ngo HH, Guo W. A mini review on renewable sources for biofuel. Bioresour Technol 2014;169:742–9. http://dx.doi.org/10.1016/j.biortech.2014.07.022.
[4] Zhao P, Shen G, Ge S, Chen Z, Yoshikawa K. Clean solid biofuel production from high moisture content waste biomass employing hydrothermal treatment. Appl Energy 2014;131:345–67. http://dx.doi.org/10.1016/j.apenergy.2014.06.038.
[5] Hoekman SK, Broch A, Warren A, Felix L, Irvin J. Laboratory pelletization of hydrochar from woody biomass. Biofuels 2014;5:651–66. http://dx.doi.org/10.1080/17597269.2015.1012693.
[6] Mäkelä M, Fraikin L, Léonard A, Benavente V, Fullana A. Predicting the drying properties of sludge based on hydrothermal treatment under subcritical conditions. Water Res 2016;91:11–8. http://dx.doi.org/10.1016/j.watres.2015.12.043.
[7] Ruyter HP. Coalification model. Fuel 1982;61:1182–7. http://dx.doi.org/10.1016/0016-2361(82)90017-5.
[8] ScienceDirect; 2016. <http://www.sciencedirect.com> [accessed 21.01.2016].
[9] Funke A, Ziegler F. Hydrothermal carbonization of biomass: a summary and discussion of chemical mechanisms for process engineering. Biofuels, Bioprod Biorefin 2010;4:160–77. http://dx.doi.org/10.1002/bbb.
[10] Mäkelä M, Benavente V, Fullana A. Hydrothermal carbonization of lignocellulosic biomass: effect of process conditions on hydrochar properties. Appl Energy 2015;155:576–84. http://dx.doi.org/10.1016/j.apenergy.2015.06.022.
[11] Sevilla M, Fuertes AB. The production of carbon materials by hydrothermal carbonization of cellulose. Carbon 2009;47:2281–9. http://dx.doi.org/10.1016/j.carbon.2009.04.026.
[12] Yu Y, Lou X, Wu H. Some recent advances in hydrolysis of biomass in hot-compressed water and its comparison with other hydrolysis methods. Energy Fuel 2008;22:46–60. http://dx.doi.org/10.1021/ef700292p.
[13] Kambo HS, Dutta A. Strength, storage, combustion characteristics of densified lignocellulosic biomass produced via torrefaction and hydrothermal carbonization. Appl Energy 2014;135:182–91. http://dx.doi.org/10.1016/j.apenergy.2014.08.094.
[14] Kambo HS, Dutta A. A comparative review of biochar and hydrochar in terms of production, physico-chemical properties and applications. Renew Sust Energy Rev 2015;45:359–78. http://dx.doi.org/10.1016/j.rser.2015.01.050.
[15] Tortosa Masià AA, Buhre BJP, Gupta RP, Wall TF. Characterising ash of biomass and waste. Fuel Process Technol 2007;88:1071–81. http://dx.doi.org/10.1016/j.fuproc.2007.06.011.
[16] Jenkins BM, Baxter LL, Miles Jr TR, Miles TR. Combustion properties of biomass. Fuel Process Technol 1998;54:17–46. http://dx.doi.org/10.1016/S0378-3820(97)00059-3.
[17] Reza MT, Lynam JG, Uddin MH, Coronella CJ. Hydrothermal carbonization: fate of inorganics. Biomass Bioenergy 2013;49:86–94. http://dx.doi.org/10.1016/j.biombioe.2012.12.004.
[18] Benavente V, Calabuig E, Fullana A. Upgrading of agro-industrial wastes by hydrothermal carbonization. J Anal Appl Pyrolysis 2015;113:89–98. http://dx.doi.org/10.1016/j.jaap.2014.11.004.
[19] Smith AM, Singh S, Ross AB. Fate of inorganic material during hydrothermal carbonisation of biomass: influence of feedstock on combustion behaviour of hydrochar. Fuel 2016;169:135–45. http://dx.doi.org/10.1016/j.fuel.2015.12.006.
[20] Lynam JG, Reza MT, Yan W, Vásquez VR, Coronella CJ. Hydrothermal carbonization of various lignocellulosic biomass. Biomass Convers Biorefin 2015;5:173–81. http://dx.doi.org/10.1007/s13399-014-0137-3.
[21] Yan W, Acharjee TC, Coronella CJ, Vasquez VR. Thermal pretreatment of lignocellulosic biomass. Environ Prog Sust Energy 2009;28:435–40. http://dx.doi.org/10.1002/ep.10385.
[22] Reza MT, Uddin MH, Lynam JG, Hoekman SK, Coronella CJ. Hydrothermal carbonization of loblolly pine: reaction chemistry and water balance. Biomass Conver Biorefin 2014;4:311–21. http://dx.doi.org/10.1007/s.13399-014-0115-9.
[23] Sermyagina E, Saari J, Kaikko J, Vakkilainen E. Hydrothermal carbonization of coniferous biomass: effect of process parameters on mass and energy yields. J Anal Appl Pyrolysis 2015;113:551–6. http://dx.doi.org/10.1016/j.jaap.2015.03.012.
[24] Gao P, Zhou Y, Meng F, Zhang Y, Liu Z, Zhang W, et al. Preparation and characterization of hydrochar from waste eucalyptus bark for hydrothermal carbonization. Energy 2016;97:238–45. http://dx.doi.org/10.1016/j.energy.2015.12.123.
[25] Kambo HS, Dutta A. Comparative evaluation of torrefaction and hydrothermal carbonization of lignocellulosic biomass for the production of solid biofuel. Energy Convers Manage 2015;105:746–55. http://dx.doi.org/10.1016/j.enconman.2015.08.031.
[26] Reza MT, Becker W, Sachsenheimer K, Mumme J. Hydrothermal carbonization (HTC): near infrared spectroscopy and partial least-squares regression for determination of selective components in HTC solid and liquid products derived from maize silage. Bioresour Technol 2014;161:91–101. http://dx.doi.org/10.1016/j.biortech.2014.03.008.
[27] Reza MT, Rottler E, Herklotz L, Wirth B. Hydrothermal carbonization (HTC) of wheat straw: influence of feedwater pH prepared by acetic acid and potassium hydroxide. Bioresour Technol 2015;182:336–44. http://dx.doi.org/10.1016/j.biortech.2015.02.024.
[28] Xu Q, Qian Q, Quek A, Ai N, Zeng G, Wang J. Hydrothermal carbonization of macroalgae and the effects of experimental parameters on the properties of hydrochars. ACS Sust Chem Eng 2013;1:1092–101. http://dx.doi.org/10.1021/sc400118f.
[29] Nurdiawati A, Srikandi N, Zaini IN, Sumida H, Yoshikawa K. Production of low-potassium solid fuel from empty fruit bunches (EFB) by employing hydrothermal treatment and water washing process. J Jpn Inst Energy 2015;94:775–80. http://dx.doi.org/10.3775/jie.94.775.
[30] Poerschmann J, Weiner B, Wedwitschka H, Baskyr I, Koehler R, Kopinke F-D. Characterization of biocoals and dissolved organic matter phases obtained upon hydrothermal carbonization of brewer's spent grain. Bioresour Technol 2014;164:162–9. http://dx.doi.org/10.1016/j.biortech.2014.04.052.
[31] Berge ND, Ro KS, Mao J, Flora JRV, Chappell MA, Bae S. Hydrothermal carbonization of municipal waste streams. Environ Sci Technol 2011;45:5696–703. http://dx.doi.org/10.1021/es2004528.
[32] Prawisudha P, Namioka T, Yoshikawa K. Coal alternative fuel production from municipal solid wastes employing hydrothermal treatment. Appl Energy 2012;90:298–304. http://dx.doi.org/10.1016/j.apenergy.2011.03.021.
[33] Basso D, Weiss-Hortala W, Patuzzi F, Castello D, Baratieri M, Fiori L. Hydrothermal carbonization of off-specification compost: a byproduct of the organic municipal waste treatment. Bioresour Technol 2015;182:217–24. http://dx.doi.org/10.1016/j.biortech.2015.01.118.
[34] Afolabi OOD, Sohail M, Thomas CPL. Microwave hydrothermal carbonization of human biowastes. Waste Biomass Valoriz 2015;6:147–57. http://dx.doi.org/10.1007/s12649-014-9333-4.
[35] Danso-Boateng E, Shama G, Wheatley AD, Martin SJ, Holdich RG. Hydrothermal carbonisation of sewage sludge: effect of process conditions on product characteristics and methane production. Bioresour Technol 2015;177:318–27. http://dx.doi.org/10.1016/j.biortech.2014.11.096.
[36] Mäkelä M, Benavente V, Fullana A. Hydrothermal carbonization of industrial mixed sludge from a pulp and paper mill. Bioresour Technol 2016;200:444–50. http://dx.doi.org/10.1016/j.biortech.2015.10.062.
[37] Jackson JE. A user's guide to principal components. New York: John Wiley & Sons Inc; 1991.
[38] Daszykowski M, Walczak B, Massart DL. Projection methods in chemistry. Chemom Intell Lab Syst 2003;65:97–112. http://dx.doi.org/10.1016/S0169-7439(02)00107-7.
[39] Geladi P. Chemometrics in spectroscopy. Part 1. Classical chemometrics. Spectrochim Acta Part B 2003;58:767–82. http://dx.doi.org/10.1016/S0584-8547(03)00037-5.
[40] Bobleter O. Hydrothermal degradation of polymers derived from plants. Prog Polym Sci 1994;19:797–841. http://dx.doi.org/10.1016/0079-6700(94)90033-7.
[41] Bach Q-V, Tran K-Q, Khalil RA, Skreiberg Ø, Seisenbaeva G. Comparative assessment of wet torrefaction. Energy Fuel 2013;27:6743–53. http://dx.doi.org/10.1021/ef401295w.
[42] Funke A, Reebs F, Kruse A. Experimental comparison of hydrothermal and vapothermal carbonization. Fuel Process Technol 2013;115:261–9. http://dx.doi.org/10.1016/j.fuproc.2013.04.020.
[43] Dahl O. Environmental management and control. 2nd ed. Helsinki: Finnish Paper Engineers' Association; 2008.
[44] Nurmesniemi H, Pöykiö R, Keiski RL. A case study of waste management at the Northern Finnish pulp and paper mill complex of Stora Enso Veitsiluoto Mills. Waste Manage (Oxford) 2007;27:1939–48. http://dx.doi.org/10.1016/j.wasman.2006.07.017.
[45] Heilmann SM, Molde JS, Timler JG, Wood BM, Mikula AL, Vozhdayev GV, et al. Phosphorus reclamation through hydrothermal carbonization of animal manures. Environ Sci Technol 2014;48:10323–9. http://dx.doi.org/10.1021/es501872k.
[46] Dai L, Tan F, Wu B, He M, Wang W, Tang X, et al. Immobilization of phosphorus in cow manure during hydrothermal carbonization. J Environ Manage 2015;157:49–53. http://dx.doi.org/10.1016/j.jenvman.2015.04.009.
[47] Vassilev SV, Baxter D, Vassileva CG. An overview of the behaviour of biomass during combustion: Part I. Phase-mineral transformations of organic and inorganic matter. Fuel 2013;112:391–449. http://dx.doi.org/10.1016/j.fuel.2013.05.043.
[48] Vassilev SV, Baxter D, Vassileva CG. An overview of the behaviour of biomass during combustion: Part II. Ash fusion and ash transformation mechanisms of biomass types. Fuel 2014;117:152–83. http://dx.doi.org/10.1016/j.fuel.2013.09.024.